Melatonin promotes sleep by activating the BK channel in *C. elegans*

Longgang Niu[a], Yan Li[a,1], Pengyu Zong[a], Ping Liu[a,2], Yuan Shui[a], Bojun Chen[a,3], and Zhao-Wen Wang[a,3]

[a]Department of Neuroscience, University of Connecticut School of Medicine, Farmington, CT 06030-3401

Edited by Richard W. Aldrich, The University of Texas at Austin, Austin, TX, and approved August 28, 2020 (received for review May 28, 2020)

Melatonin (Mel) promotes sleep through G protein-coupled receptors. However, the downstream molecular target(s) is unknown. We identified the *Caenorhabditis elegans* BK channel SLO-1 as a molecular target of the Mel receptor PCDR-1-. Knockout of *pcdr-1*, *slo-1*, or *homt-1* (a gene required for Mel synthesis) causes substantially increased neurotransmitter release and shortened sleep duration, and these effects are nonadditive in double knockouts. Exogenous Mel inhibits neurotransmitter release and promotes sleep in wild-type (WT) but not *pcdr-1* and *slo-1* mutants. In a heterologous expression system, Mel activates the human BK channel (hSlo1) in a membrane-delimited manner in the presence of the Mel receptor MT_1 but not MT_2. A peptide acting to release free Gβγ also activates hSlo1 in a MT_1-dependent and membrane-delimited manner, whereas a Gβλ inhibitor abolishes the stimulating effect of Mel. Our results suggest that Mel promotes sleep by activating the BK channel through a specific Mel receptor and Gβλ.

melatonin | BK channel | PCDR-1 | melatonin receptor | sleep

Melatonin (Mel) is generally known as a hormone of darkness or a sleep hormone because it plays a pivotal role in sleep. In the human brain, Mel is secreted by the pineal gland with low levels during the day and high levels at night. This rhythmic secretion of Mel is under the control of neurons in the suprachiasmatic nucleus (SCN), which is the site of a circadian master clock, and receives synaptic inputs from photosensitive neurons in the retina (1–3). Many people take Mel supplements as a sleep aid.

Mel is believed to produce its sleep effect through Mel receptors. Two Mel receptors exist in mammals: MT_1 and MT_2 (4). Experiments with knockout mice indicate that MT_1 and MT_2 deficiencies compromise rapid eye movement (REM) sleep and non-REM sleep, respectively (5). MT_1 signaling is also important to circadian rhythmic expression of several clock genes (6, 7). However, it is unclear whether MT_1 and MT_2 play similar roles in humans, mainly due to a lack of sufficiently selective receptor agonists and antagonists (4, 8). Although it is well established that MT_1 and MT_2 function through G_i-type G proteins (9), the downstream molecular targets leading to its sleep-promoting effect remain mysterious. Protein interactome mining indicates that MT_1 but not MT_2 is an integral component of a presynaptic protein complex (10), but the physiological functions of presynaptic MT_1 are undetermined.

The BK channel is a large-conductance potassium channel gated by membrane voltage and cytosolic Ca^{2+}. BK channels are ubiquitously expressed in the nervous system where they colocalize with voltage-gated Ca^{2+} channels at presynaptic sites of neurons and play a major role in downregulating neurotransmitter release (11–13). Results of previous studies indicate that the BK channel may play important roles in circadian behaviors. In mice, expression level of the BK channel in the SCN oscillates according to daily light and dark cycles (14), and this oscillation regulates the SCN neuron firing rate and circadian behavioral rhythms (15). In rats, the BK channel serves to inhibit spontaneous Ca^{2+} oscillations in pinealocytes (16). In flies, inhibition of the BK channel promotes wakefulness (17). However, it is unknown whether the BK channel plays a role in sleep.

C. elegans goes through four larval stages (L1–L4) before becoming an adult. A behavioral quiescence period, known as lethargus, exists between consecutive larval stages and between L4 and adult. Lethargus is considered a sleep state of worms because it bears major behavioral and molecular similarities to sleep states of other species (18–23). During the lethargus, behavioral quiescence is frequently interrupted by brief movements (19). Although *C. elegans* also produces Mel (24) and has one putative Mel receptor (F59D12.1/PCDR-1) (25), neither Mel nor the receptor has been implicated in the lethargus.

We have been using a forward genetics approach to identify proteins important to in vivo functions of SLO-1, the *C. elegans* BK channel (26–28). Here, we report that PCDR-1, one of the proteins identified from our genetic screen, is an indispensable molecule for SLO-1 physiological function in neurons, and that it allows Mel to promote sleep by activating SLO-1. Furthermore, we found that the human BK channel hSlo1 is activated by Mel through MT_1 but not MT_2, and this effect of MT_1 occurs through a membrane-delimited mechanism requiring Gβγ subunits and may be produced by Mel at concentrations ($EC_{50} < 1$ nM) within the reported Mel concentration range in the human cerebrospinal fluid (29). Our results suggest that BK channels may play an evolutionarily conserved role in mediating the sleep effect of Mel.

Results

Neuronal SLO-1 Function Depends on PCDR-1. In an unbiased genetic screen with *C. elegans* for mutants that ameliorate a sluggish phenotype caused by a hyperactive or gain-of-function (*gf*) SLO-1 (26), we isolated a mutant *zw82*, which was mapped to a gene (*F59D12.1*) encoding a G protein-coupled receptor (GPCR). F59D12.1 was initially predicted as a Mel receptor based on

Significance

Melatonin (Mel) promotes sleep through G protein-coupled Mel receptors. However, the downstream molecular target(s) of the Mel receptors to produce the sleep effect remains enigmatic. The study shows that a potassium channel, the BK channel, plays a role in sleep and that Mel promotes sleep by activating this channel through a specific Mel receptor.

Author contributions: L.N., B.C., and Z.-W.W. designed research; L.N., Y.L., P.Z., P.L., Y.S., and B.C. performed research; L.N., P.Z., and P.L. analyzed data; and Z.-W.W. wrote the paper.

The authors declare no competing interest.

This article is a PNAS Direct Submission.

[1]Present address: Lunenfeld-Tanenbaum Research Institute, Mount Sinai Hospital, Toronto, Canada.

[2]Present address: Department of Pathophysiology, School of Basic Medicine and Tongji Medical College, Huazhong University of Science and Technology, Wuhan, China.

[3]To whom correspondence may be addressed. Email: bochen@uchc.edu or zwwang@uchc.edu.

This article contains supporting information online at https://www.pnas.org/lookup/suppl/doi:10.1073/pnas.2010928117/-/DCSupplemental.

First published September 21, 2020.

phylogenetic analyses (25) but was recently named PCDR-1 (pathogen clearance-defective receptor 1) because mutations of the gene are associated with a pathogen clearance defect phenotype (30). PCDR-1 shows significant sequence homology to human MT_1 and MT_2 receptors (*SI Appendix*, Fig. S1*A*). In *zw82*, cysteine 148, which is located in a putative transmembrane domain of PCDR-1, is mutated to tyrosine (*SI Appendix*, Fig. S1 *A* and *B*).

Neurotransmitter release is increased in the *slo-1* loss-of-function *(lf)* mutant but decreased in the *slo-1(gf)* mutant (26, 31). To determine whether and how PCDR-1 regulates the SLO-1 function, we assessed the role of PCDR-1 in neurotransmitter release by analyzing evoked postsynaptic currents (ePSCs) and miniature postsynaptic currents (minis) at the neuromuscular junction. To avoid potential ambiguities associated with the missense mutation of *zw82*, we used two putative *pcdr-1* null alleles, *gk1122* and *gk1000* (*SI Appendix*, Fig. S1*B*) from the Caenorhabditis Genetics Center. Compared with WT, both mutants showed larger ePSC amplitudes and higher mini frequencies without a change in the mean amplitude of minis (Fig. 1 *A* and *B*). These phenotypes are similar to those of *slo-1(lf)* and were not aggravated in the *slo-1(lf);pcdr-1(lf)* double mutant (Fig. 1 *A* and *B*). In the

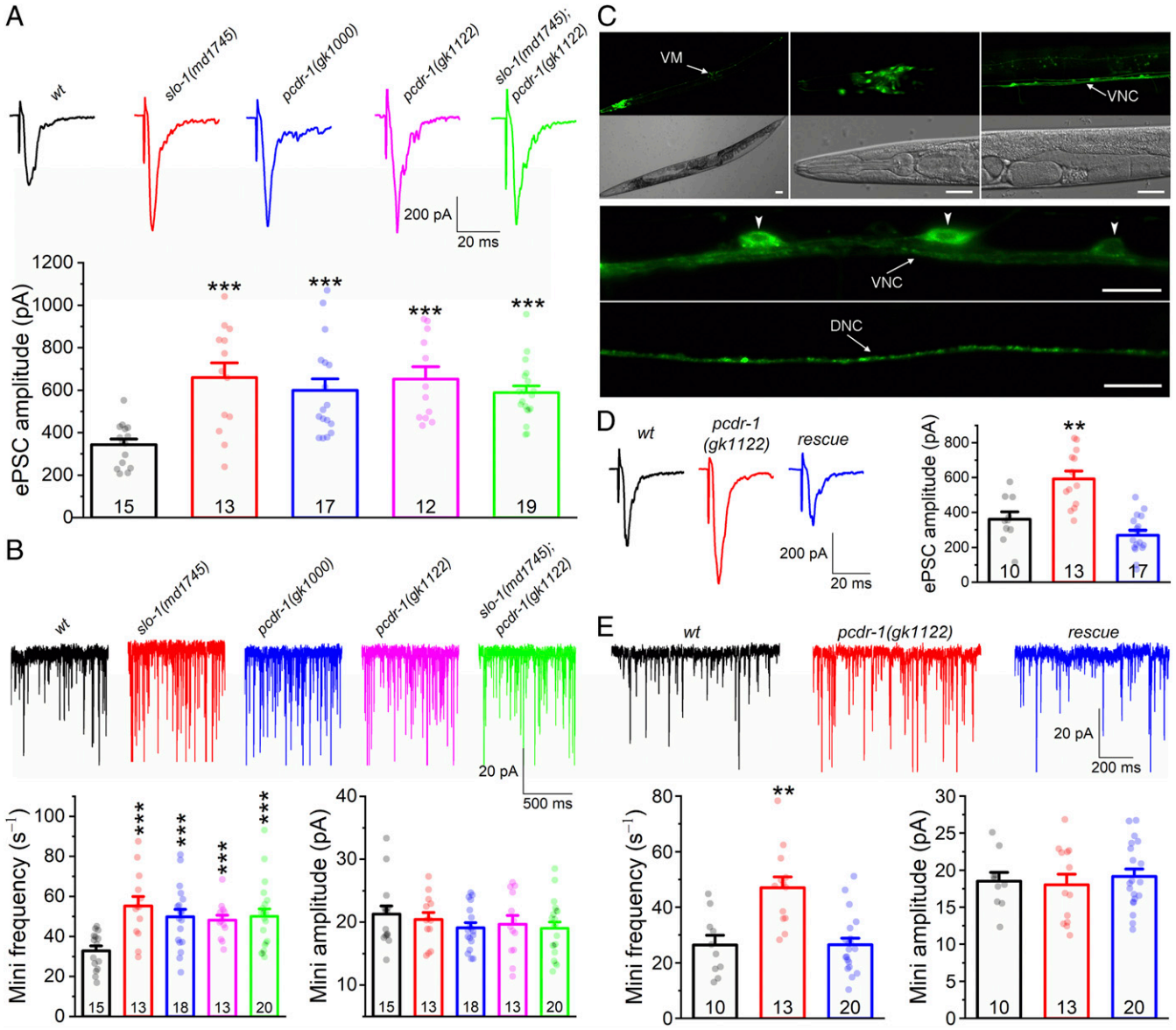

Fig. 1. PCDR-1 and SLO-1 act together to regulate neurotransmitter release. (*A* and *B*) Loss-of-function mutations of *pcdr-1* and *slo-1* similarly augmented the amplitude of ePSCs (*A*) and the frequency of minis (*B*) at the neuromuscular junction, and these mutant effects were nonadditive in the *slo-1;pcdr-1* double mutant. (*C*) PCDR-1 expression and subcellular localization patterns. *Top*, *pcdr-1* is expressed in many head neurons, ventral nerve cord (VNC) motor neurons, and vulval muscles (VMs) based on the expression of the GFP reporter under the control of the *pcdr-1* promoter. Shown are corresponding dark field and differential interference contrast images of the entirety (*Left*), the head (*Middle*), and the midportion (*Right*) of a worm (Scale bar, 20 μm.) *Bottom*, dark field images of the VNC (indicated by an arrow) and dorsal nerve cord (DNC) (indicated by an arrow) of transgenic worms expressing a PCDR-1::GFP fusion protein under the control of the pan-neuronal *rab-3* promoter (P*rab-3*) (scale bar, 10 μm.) Arrow heads indicate motor neuron cell bodies. (*D* and *E*) The synaptic phenotypes of the *pcdr-1* mutant at the neuromuscular junction were completely rescued by presynaptic expression of WT PCDR-1 under the control of P*rab-3*. The numbers inside the bar graphs indicate sample sizes. The ** and *** symbols indicate statistically significant differences compared with WT at $P < 0.01$ and $P < 0.001$ levels, respectively (one-way ANOVA with Tukey's post hoc test).

slo-1(gf) mutant, both the amplitude of the ePSCs and the frequency of the minis were greatly decreased compared with WT, and these phenotypes were eliminated in the *slo-1(gf);pcdr-1(gk1122)* double mutant (*SI Appendix*, Fig. S2). The mutant effects of *pcdr-1(lf)* on synaptic transmission did not result from a change in either expression or subcellular localization of SLO-1 (*SI Appendix*, Fig. S3). Taken together, these results suggest that neuronal SLO-1 function depends on PCDR-1.

To determine the expression pattern of *pcdr-1*, we expressed a green fluorescent protein (GFP) reporter in worms under the control of the *pcdr-1* promoter. In transgenic worms, the GFP signal was detected in many neurons, including ventral cord motor neurons and head neurons but not in body-wall muscles (Fig. 1*C*), suggesting that PCDR-1 likely functions presynaptically to regulate synaptic transmission. Consistently, the neuromuscular synaptic phenotypes of *pcdr-1(lf)* could be rescued by expressing WT PCDR-1 in neurons alone (Fig. 1 *D* and *E*).

PCDR-1 Is a Mel Receptor. Although *C. elegans* produces Mel (24, 32) and PCDR-1 has been predicted as a Mel receptor (25), no Mel receptor has been experimentally confirmed in worms. We examined the possibility of PCDR-1 being a Mel receptor by testing the effects of Mel and Mel receptor antagonists on ePSCs and minis. In WT worms, Mel (100 nM) reduced both the amplitude of ePSCs and the frequency of minis without an effect on the mean amplitude of minis (Fig. 2 *A* and *B*). These effects of Mel on synaptic transmission are similar to those of SLO-1(*gf*) (*SI Appendix*, Fig. S2). In *pcdr-1(lf)* and *slo-1(lf)* mutants, however, Mel showed no effect on either ePSCs or minis (Fig. 2 *A* and *B*). These results suggest that PCDR-1 is a Mel receptor that inhibits neurotransmitter release through SLO-1.

To determine whether acute blockade of PCDR-1 alters synaptic transmission, we first tested the effect of the nonselective Mel receptor antagonist luzindole (3) because pretreatment with luzindole counteracts an inhibitory effect of exogenous Mel on worm locomotion (24). However, application of luzindole (1 μM) to the bath solution inhibited both the amplitude of ePSCs and the frequency of minis (*SI Appendix*, Fig. S4), which cannot be explained by a blocking effect on PCDR-1. We, then, tested the effect of the MT_2-selective antagonist 4-P-PDOT (3). In WT worms, 4-P-PDOT increased both the amplitude of ePSCs and the frequency of minis without altering the mean amplitude of minis (Fig. 2 *C* and *D*). These effects of 4-P-PDOT on synaptic transmission are similar to those of *pcdr-1(lf)* and *slo-1(lf)* mutants (Fig. 1 *A* and *B*). In contrast, 4-P-PDOT showed no effect on synaptic transmission in the *pcdr-1(lf)* mutant (Fig. 2 *C* and *D*), suggesting that it augments synaptic transmission by blocking PCDR-1. We, subsequently, tested the effect of the MT_2 receptor agonist IIK7 (3) (300 nM) in WT but did not detect any effect on either ePSCs or minis (*SI Appendix*, Fig. S4). Finally, we tested the Mel precursor serotonin (100 nM) and found that it did not alter either ePSCs or minis (*SI Appendix*, Fig. S5). Collectively, our results suggest that PCDR-1 is a Mel receptor with pharmacological properties distinct from mammalian MT_1 and MT_2.

Endogenous Mel Acts on PCDR-1. Mel is synthesized from serotonin through sequential actions of serotonin *N*-acetyltransferase (SNAT) and hydroxyindole-O-methyltransferase (HIOMT) (33) (Fig. 3*A*). The worm HIOMT is encoded by *homt-1* (24). To determine whether the function of PCDR-1 depends on endogenous Mel, we created a *homt-1(lf)* strain using the CRISPR/Cas9 approach and determined the effect of HOMT-1 deficiency on synaptic

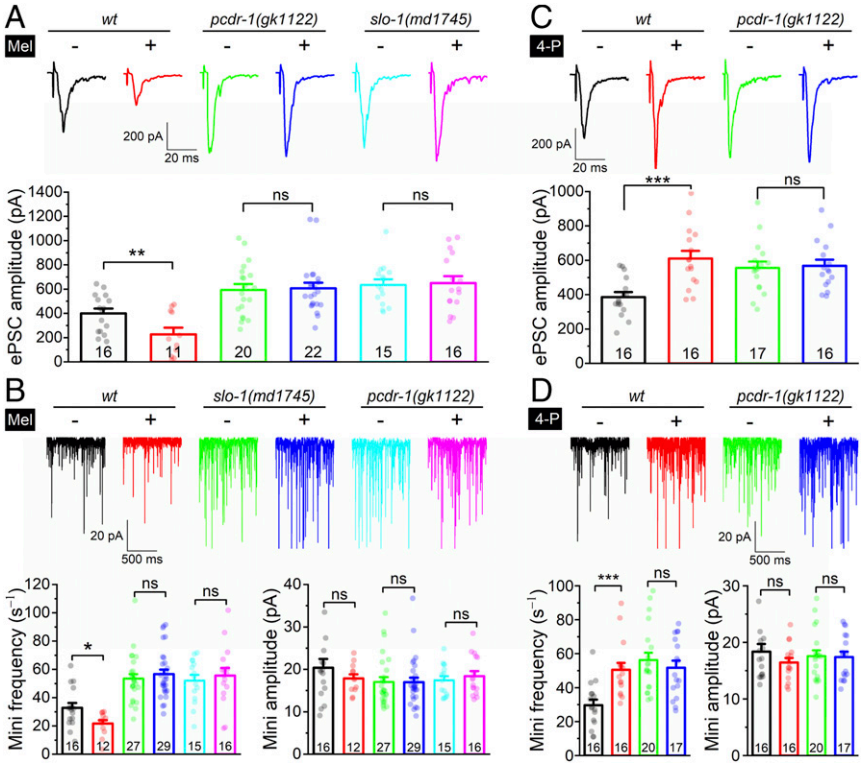

Fig. 2. PCDR-1 is activated by Mel but blocked by *cis*-4-phenyl-2-propionamidotetralin (4-P-PDOT). (*A* and *B*) Mel (100 nM) reduced the amplitude of ePSCs and the frequency of minis without altering the mean amplitude of minis in WT but had no effect in *pcdr-1* and *slo-1* mutants. (*C* and *D*) 4-P-PDOP (4-P, 100 nM) increased the amplitude of ePSCs and the frequency of minis without altering the mean amplitude of minis in WT but had no effect in the *pcdr-1* mutant. The numbers inside the bar graphs indicate sample sizes. The asterisks indicate statistically significant differences (*$P < 0.05$; **$P < 0.01$; ***$P < 0.001$) whereas "ns" stands for "no significant difference" compared with the vehicle control group (unpaired *t* test).

transmission. Compared with WT, *homt-1(lf)* worms showed a 55% increase in the amplitude of ePSCs and a 102% increase in the frequency of minis, and these synaptic phenotypes were nonadditive with those of *pcdr-1(lf)* (Fig. 3 *B* and *C*), suggesting that HOMT-1 and PCDR-1 act in the same pathway in regulating neurotransmitter release and that the function of PCDR-1 depends on endogenous Mel.

To determine the source of Mel for activating PCDR-1, we assessed the expression pattern of *homt-1* by expressing the GFP reporter under the control of the *homt-1* promoter. In transgenic worms, GFP expression was observed in the pharynx, intestine, and two neurons in the tail (DVB and PVT) (Fig. 3 *D* and *E*). While DVB is a γ-aminobutyric acid (GABA)ergic motor neuron that innervates enteric muscles (34), PVT is an interneuron that projects along the ventral nerve cord to the nerve ring (35) (https://www.wormatlas.org/). Because both the intestine and the neurite of PVT are close to ventral cord motor neurons (Fig. 3*E*), we determined whether intestine- or PVT-targeted

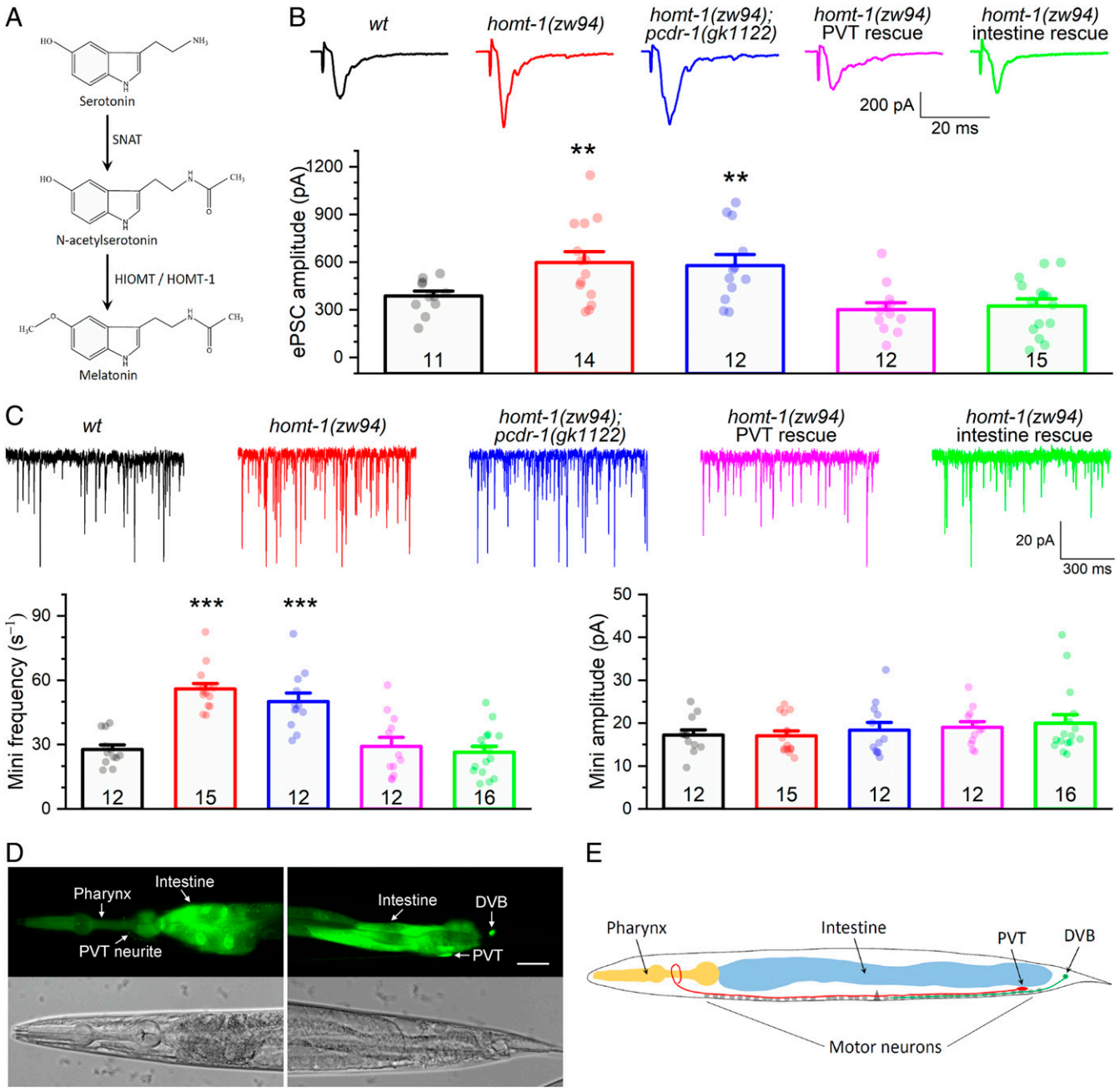

Fig. 3. PCDR-1 synaptic function depends on endogenous Mel. (*A*) Mel synthesis pathway. (*B* and *C*) Loss-of-function mutation of *homt-1* augmented the amplitude of ePSCs and the frequency of minis without altering the mean amplitude of minis at the neuromuscular junction. These effects were nonadditive with those of the *pcdr-1* mutation and could be rescued completely by expressing WT HOMT-1 in either the PVT neuron using the *zig-2* promoter or the intestine using the *inx-16* promoter. The numbers inside the bar graphs indicate sample sizes. The ** and *** indicate statistically significant differences at $P < 0.01$ and $P < 0.001$ levels, respectively, compared with WT (one-way ANOVA with Tukey's post hoc test). (*D*) *homt-1* is expressed in the intestine, PVT neuron, DVB neuron, and the pharynx based on the expression of the GFP reporter under the control of the *homt-1* promoter. (*E*) Diagram showing spatial relations of ventral cord motor neurons, the intestine, PVT neuron, and DVB neuron.

expression of WT HOMT-1 can rescue *homt-1(lf)* with respect to its synaptic phenotypes. We found that expression of WT HOMT-1 in either the intestine or the PVT neuron obliterated the synaptic phenotypes of *homt-1(lf)* (Fig. 3 *B* and *C*), suggesting that Mel release from both the intestine and the PVT regulates neurotransmitter release from ventral cord motor neurons. These results are consistent with a hormonal effect of Mel because ventral cord motor neurons do not receive direct synaptic inputs from either the PVT or the intestine.

Mel Promotes Sleep through PCDR-1 and SLO-1. We then determined whether the Mel/PCDR-1/SLO-1 pathway plays a role in sleep. We analyzed the effects of mutations of *slo-1*, *pcdr-1*, and *homt-1* on the sleep behavior between L4 and adult using a

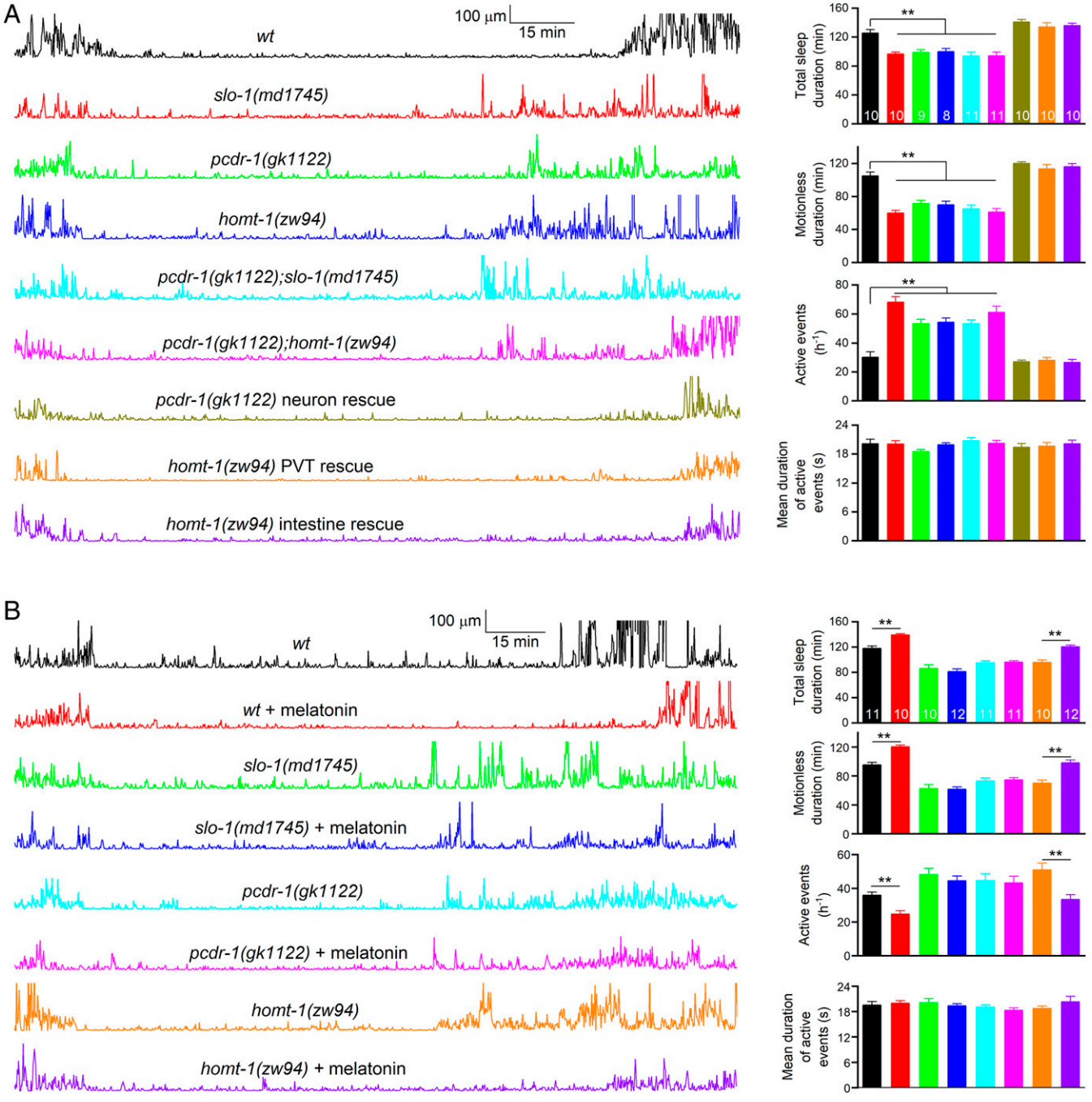

Fig. 4. Mel promotes sleep through PCDR-1 and SLO-1. (*A*) Compared with WT, loss-of-function mutants of *slo-1*, *pcdr-1*, and *homt-1* showed shorter durations of both total sleep and motionless sleep, and higher frequencies of active events during sleep. This phenotype of *pcdr-1* could be rescued by expressing WT PCDR-1 in neurons under the control of the *rab-3* promoter and that of *homt-1* by expressing WT HOMT-1 in either the PVT neuron using the *zig-2* promoter or the intestine using the *inx-16* promoter. (*B*) Exogenous Mel (10 μM) prolonged the durations of both total sleep and motionless sleep and reduced the frequency of active events during sleep in WT and the *homt-1* mutant but had no effect in *slo-1* and *pcdr-1* mutants. The numbers inside the bar graphs indicate sample sizes. The ** indicate statistically significant differences ($P < 0.01$) compared with the vehicle control group based on either one-way ANOVA with Tukey's post hoc test (*A*) or unpaired *t* test (*B*).

custom-made sleep chamber (*SI Appendix*, Fig. S6). In WT worms, the total sleep duration, the motionless sleep duration, and the frequency of active events during sleep were 125 ± 4.83, 105 ± 4.65 min, and 30 ± 3.70/h, respectively (Fig. 4*A*). Compared with WT, mutants of *slo-1(lf)*, *pcdr-1(lf)*, and *homt-1(lf)* showed 20–43% decreases in both the total and the motionless sleep durations but an approximately twofold increase in the frequency of active events (Fig. 4*A*). These mutant phenotypes were not aggravated in *pcdr-1(lf);slo-1(lf)* and *pcdr-1(lf);homt-1(lf)* double mutants (Fig. 4*A*). The sleep phenotypes of *pcdr-1(lf)* could be rescued completely by expressing WT PCDR-1 specifically in neurons and those of *homt-1(lf)* by expressing WT HOMT-1 specifically in either PVT neuron or intestine (Fig. 4*A*). These results suggest that HOMT-1-dependent release of endogenous Mel can enhance sleep through PCDR-1 and SLO-1. We also tested whether SLO-2, a paralog of SLO-1 (36) with a regulatory role in neurotransmitter release (37), is important to sleep. We observed similar sleep behaviors between the WT and a putative *slo-2* null mutant (38) (*SI Appendix*, Fig. S7), suggesting that SLO-2 does not play a role in sleep.

Subsequently, we tested whether exogenous Mel may enhance worm sleep. Compared with the vehicle control groups, Mel (100 nM) enhanced sleep as indicated by increased durations of total sleep and motionless sleep in the WT and *homt-1(lf)* mutant (Fig. 4*B*). In contrast, Mel had no effect on the sleep behaviors when applied to *slo-1(lf)* and *pcdr-1(lf)* mutants (Fig. 4*B*). These results indicate that both PCDR-1 and SLO-1 are required for the sleep-enhancing effects of exogenous Mel.

Finally, we tested whether light and darkness conditions may have different effects on Mel's action because the BK channel level in mammals varies with the day/night cycles (14). We subjected worms to either a darkness or an illuminated condition (from standard fluorescence ceiling lights) for 16–22 h prior to recording ePSCs and minis at the neuromuscular junction. The light intensities were 1.02 and 0.69 μW/mm^2 at 473-nm and 635-nm wavelengths, respectively, at the worm culture plate location. Both the amplitude of ePSCs and the frequency of minis were enhanced by the light exposure. Treatment with Mel (100 nM) inhibited ePSC amplitude and mini frequency in worms exposed to both the dark and light conditions. The inhibitory effect on ePSCs was greater in the darkness-exposed worms (ePSC amplitude reduction 66% versus 22%), although the difference did not reach statistical significance ($P = 0.058$) (*SI Appendix*, Fig. S8). These results suggest that SLO-1 expression might be down-regulated by light.

Mel Activates hSlo1 through MT$_1$. We considered whether mammalian BK channels are also activated by Mel. We started by testing the effect of Mel on macroscopic currents in inside–out patches from *Xenopus* oocytes coexpressing human hSlo1 and mouse MT$_1$. In these experiments, Mel (100 nM) was included in the pipette solution, and macroscopic currents were induced by voltage steps from −80 mV to +180 mV at 20-mV intervals. The currents were converted to conductance (G) to quantify V_{50} from a normalized G-voltage (V) relationship. Mel caused a significant decrease in the voltage for half-maximal channel activation (V_{50}) compared with the vehicle control in patches coexpressing hSlo1 and MT$_1$ but not in patches expressing hSlo1 alone (*SI Appendix*, Fig. S9 *A* and *B*). These results suggest that Mel can activate hSlo1 in a MT$_1$-dependent manner.

We, then, performed single-channel recordings on inside–out patches containing only one channel to determine whether Mel may activate hSlo1 through MT$_1$ and MT$_2$. Compared with the vehicle control, inclusion of Mel (100 nM) in the pipette solution caused a large leftward shift in the open probability (P_o)-V relationship in patches coexpressing hSlo1 and mouse MT$_1$ (V_{50} 22.25 ± 3.28 versus −2.88 ± 3.57 mV) (Fig. 5*A*) but not in patches expressing either hSlo1 alone or hSlo1 and human MT$_2$ (*SI Appendix*, Fig. S10 *A* and *B*). Mel did not alter hSlo1 single-channel conductance in patches coexpressing hSlo1 and MT$_1$ as indicated by similar single-channel current (I)-V relationships between the control and the Mel groups (Fig. 5*A*). These results indicate that Mel can activate hSlo1 through MT$_1$ but not MT$_2$ and that the increased hSlo1 activity results from an increased P_o. To determine how Mel increases P_o in the presence of MT$_1$, we analyzed dwell times of open and closed events at +10-mV holding voltage. We found that both the open and the closed dwell times could be fit by two exponential terms (τ1 and τ2) and that Mel augmented hSlo1 P_o mainly by prolonging the τ2 of open events and reducing the τ2 of closed events (Fig. 5*B*).

We next tested the effect of Mel on hSlo1 P_o at different Ca^{2+} concentrations. Increasing concentrations of Ca^{2+} were applied to the cytosolic surface of inside–out patches coexpressing hSlo1 and MT$_1$ at a constant holding voltage. Compared with the vehicle control, Mel (100 nM) caused significant increases in hSlo1 P_o at all of the tested Ca^{2+} concentrations that were ≥3 μM (Fig. 5*C*), which indicates that MT$_1$ activation increases hSlo1 apparent Ca^{2+} sensitivity.

The concentration of Mel used in the experiments described above (100 nM) was chosen based on what has been commonly used in in vitro experiments. Because physiological concentrations of Mel might be much lower than 100 nM, we tested the effects of different concentrations of Mel on macroscopic currents in outside–out patches coexpressing hSlo1 and MT$_1$. Asymmetrical K^+ solutions were used in these experiments with the patch held constant at −80 mV (equal to the K^+ equilibrium potential). Perfusion of Mel to the extracellular side of the patch membrane at increasing concentrations (10 pM to 10 μM in logarithmic increments) caused concentration-dependent increases in outward currents. Fitting the concentration-response data to Hill's equation gave rise to a curve with an EC_{50} of 0.77 ± 0.09 nM (Fig. 5*D*). These results indicate that Mel can produce its stimulatory effect on hSlo1 at concentrations much lower than 100 nM.

MT$_1$ Activates hSlo1 through Gβγ. To determine whether and how a G protein is involved in the activation of hSlo1 by MT$_1$, we tested the effect of mSIRK, a peptide that dissociates the trimeric G proteins into Gα and Gβγ subunits without inducing guanosine diphosphate/guanosine triphosphate (GDP/GTP) exchange in the Gα subunit (39). In inside–out patches coexpressing hSlo1 and MT$_1$, application of mSIRK to the bath solution augmented hSlo P_o without an effect on single-channel conductance (Fig. 6*A*). The effect of mSIRK on P_o was nonadditive with that of Mel (100 nM in the pipette solution) and mainly due to an increased τ2 of open events and a decreased τ2 of closed events (Fig. 6 *A* and *B*). This effect is similar to that of Mel, which also increased P_o by increasing τ2 of open events and decreasing τ2 of closed events. These results suggest that mSIRK and Mel activate hSlo1 through a common mechanism, presumably through the release of free Gβγ subunits.

In contrast, mSIRK had no effect on the P_o in patches expressing hSlo1 alone (*SI Appendix*, Fig. S11). This result, in combination with the result described above, suggests that MT$_1$ might localize G proteins to the vicinity of hSlo1 to allow G protein-mediated channel activation. To obtain further evidence in support of the role of Gβγ subunits, we determined whether inclusion of gallein, a Gβγ inhibitor (40, 41), in the bath solution can prevent the stimulatory effect of Mel on channel activities in inside–out patches coexpressing MT$_1$ and hSlo1. Indeed, gallein obliterated the stimulatory effect of Mel on hSlo1 (Fig. 6*C*). Collectively, our results indicate that Mel activates hSlo1 through MT$_1$-dependent release of free Gβγ subunits.

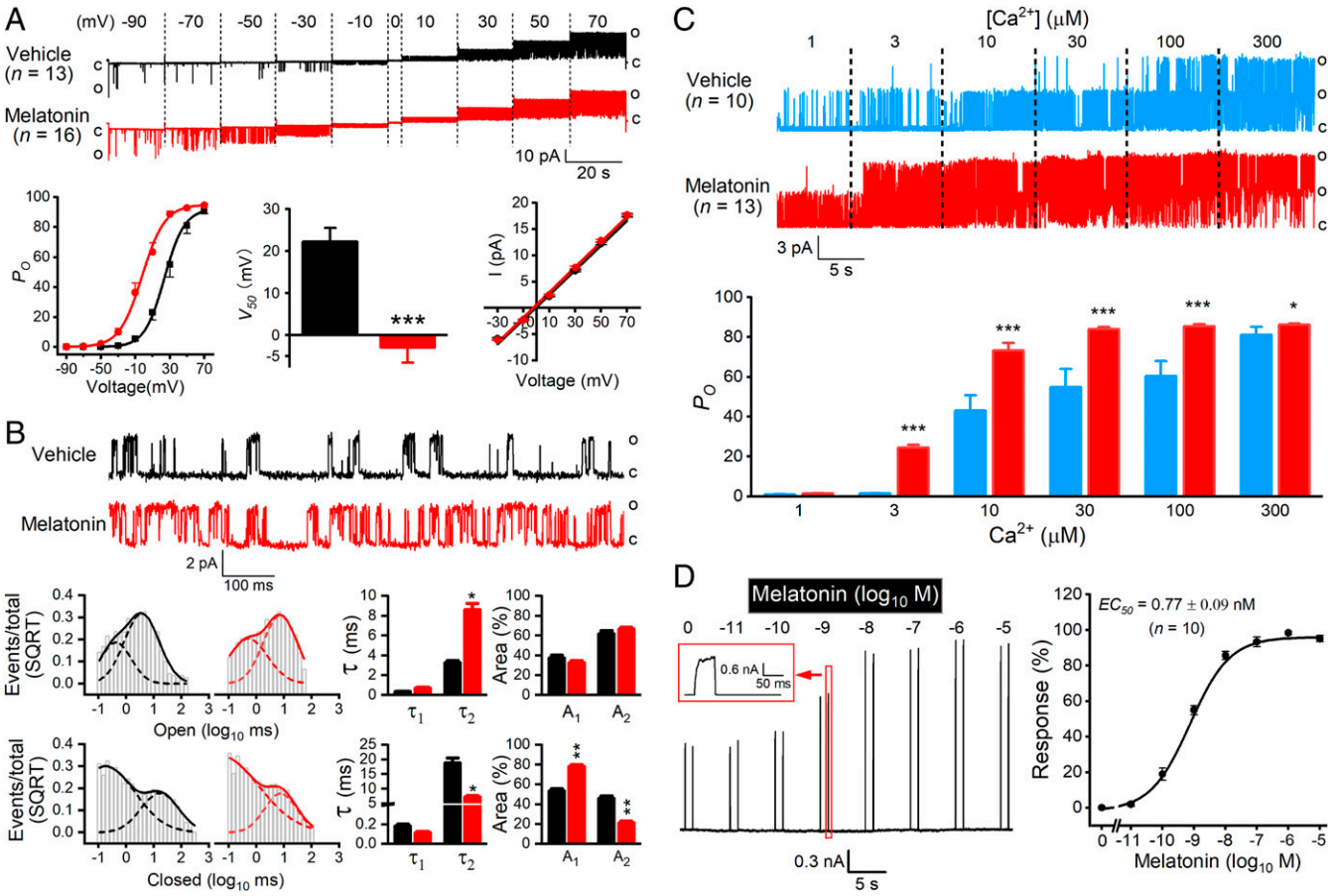

Fig. 5. Mel augments hSlo1 single-channel open probability (P_o) in isolated membrane patches coexpressing human Slo1 (hSlo1) and mouse MT_1. (*A*) Mel (100 nM) increased hSlo1 P_o without altering single-channel current amplitudes in inside–out patches containing only one channel (symmetrical K^+ solutions). Shown are sample current traces, the open probability (P_o) voltage (V) relationships, the voltage for half-maximal channel activation (V_{50}), and the current (I)-V relationships. Single-channel conductance (quantified from the I-V relationships) was 237.8 ± 5.3 pS in control and 242.1 ± 2.3 in Mel. (*B*) Mel prolonged the τ2 of open events and reduced the τ2 of closed events as determined by fitting open and closed times of hSlo1 at the +10-mV step in *A*. (*C*) Mel increased hSlo1 Ca^{2+} sensitivity. Increasing concentrations of Ca^{2+} were applied to the cytosolic side of inside–out patches (containing either one or two hSlo1 channels) held constantly at +20 mV. In *A*–*C*, the asterisks indicate statistically significant differences compared with the vehicle control group (*$P < 0.05$; **$P < 0.01$; ***$P < 0.001$, unpaired t test). (*D*) Mel increased hSlo1 activity in a concentration-dependent manner in outside–out patches containing multiple channels (asymmetrical K^+ solutions). Increasing concentrations of Mel (two applications at each concentration) were applied to the extracellular side of the patch held at −80 mV (equal to the K^+ equilibrium potential) through perfusion. hSlo1 currents were induced by stepping to +20 mV (50 ms). Shown are a sample current trace (with one Mel-induced current response displayed at an expanded time scale) and the Mel concentration—response curve fitted to the Hill's equation $E = E_{max}/(1 + (EC_{50}/A))^{nH}$, where E is the observed response and nH is the Hill coefficient reflecting the slope of the curve.

Discussion

The present study shows that the BK channel is a molecular target through which Mel promotes sleep and that Mel activates the channel through PCDR-1 in worms and MT_1 in mammals. Our results support a model in which a Mel receptor localizes a specific type of G protein to the BK channel, and binding of Mel to the receptor causes the release of free Gβγ subunits to activate the channel (Fig. 7). Our results also suggest that the BK channel is a key molecular target for Mel to produce its sleep-promoting effect in worms and that it might play a similar role in mammals. These conclusions are supported by the similar and nonadditive effects of *slo-1* and *pcdr-1* mutations on neurotransmitter release and sleep behavior in *C. elegans* and by MT_1-dependent activation of hSlo1 in a membrane-delimited manner in the *Xenopus* oocyte heterologous expression system. The putative roles of MT_1 in neurotransmitter release and sleep are also in agreement with the earlier reports that MT_1 is a molecular component of presynaptic protein complexes (10) and that both sleep and circadian rhythmic expression of clock proteins depend on MT_1 (5–7) in mice.

Sleep in *C. elegans* is a global state with the majority of neurons showing reduced activities during sleep (42). However, some neurons are active during sleep, including sleep-promoting neurons (42). Among the sleep-promoting neurons, RIS plays a pivotal role in sleep onset by releasing FLP-11, a neuropeptide, and GABA (43, 44), and its activity is regulated by interneurons, such as the bilateral pairs of PVC and RIM interneurons (45). While PVC activates RIS, RIM may either activate or inhibit RIS depending on RIM's activity level (45). How might SLO-1 contribute to sleep? One possibility is that Mel may activate SLO-1 in many neurons to produce a global inhibitory effect. Another possibility is that SLO-1 activation in inhibitory neurons presynaptic to RIS may promote sleep through a disinhibitory effect. A third possibility is that SLO-1 functions in wake-promoting neurons, such as those in the RMG circuit (46), to reduce their antagonistic effects on sleep. How exactly SLO-1 functions in sleep can potentially be addressed by analyzing the effects of cell-targeted knockdown of *slo-1* or *pcdr-1* on RIS activity and sleep behavior.

In flies, octopamine promotes wakefulness by inhibiting the BK channel (17). Octopamine is also a signaling molecule in

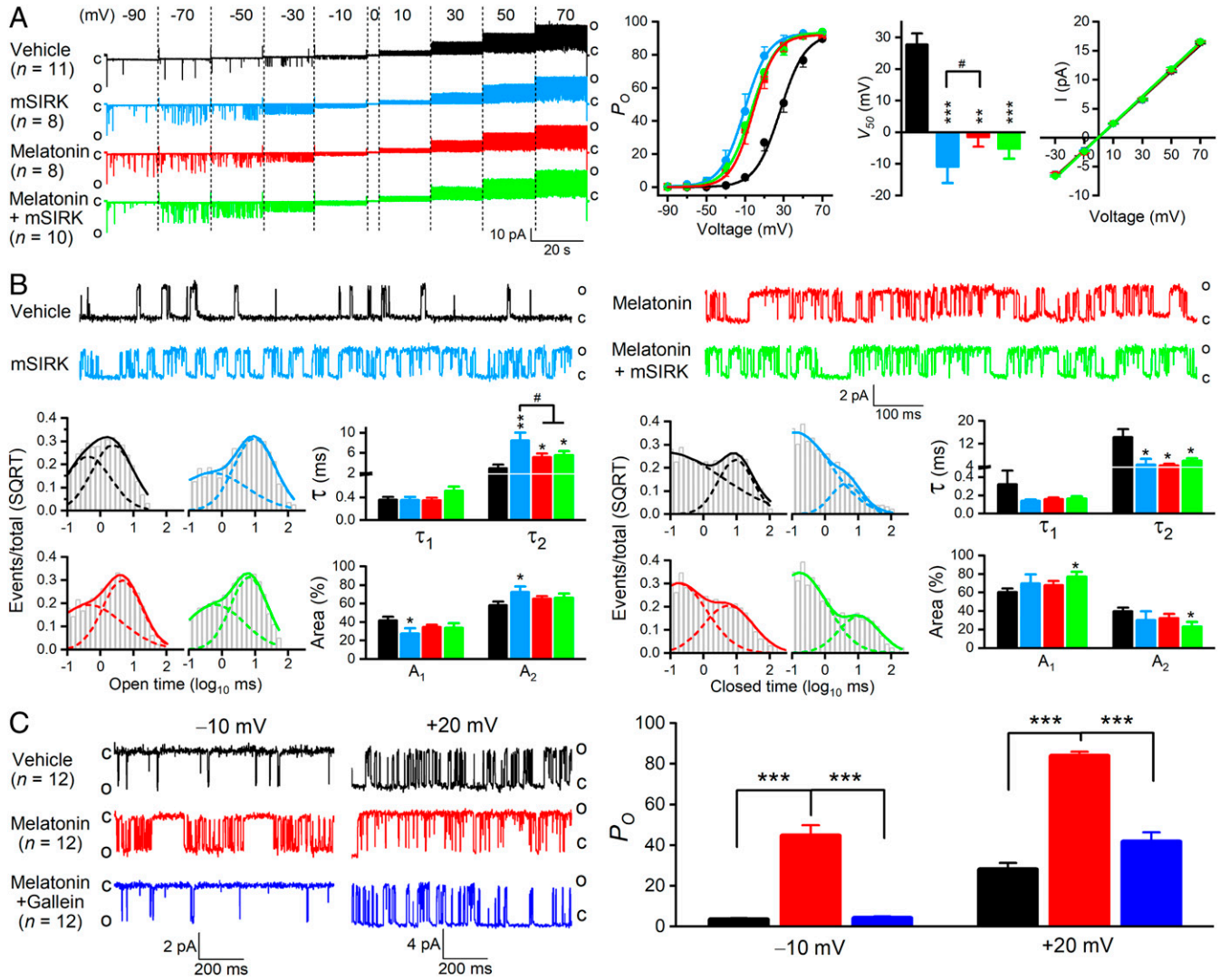

Fig. 6. Mel activates hSlo1 through Gβγ subunits. (*A*) mSIRK increased hSlo1 P_o, and this effect was nonadditive with that of Mel. Mel (100 nM) was included in the pipette solution whereas mSIRK (10 μM) was added to the bath solution. (*B*) mSIRK prolonged the τ2 of open events and reduced the τ2 of closed events as determined from analyzing the data at +10 mV in *A*. The asterisks indicate statistically significant differences (*$P < 0.05$; **$P < 0.01$; ***$P < 0.001$) compared with the vehicle control group whereas the pound sign (#) indicates a statistically significant difference between the indicated groups (one-way ANOVA with Tukey's post hoc test). (*C*) Gallein blocked the stimulatory effect of Mel on hSlo1. Mel (100 nM) was included in the pipette solution whereas gallein (10 μM) was applied to the bath solution. The control had dimethyl sulfoxide (vehicle) in both the pipette and the bath solutions. *** indicate a statistically significant difference ($P < 0.001$, one-way ANOVA with Tukey's post hoc test). All recordings were from inside–out patches coexpressing hSlo1 and MT_1 with only one channel.

worms (47). The contrasting effects of octopamine in flies and Mel in worms suggest that the BK channel might help to switch between sleep and wake states depending on the levels of octopamine and Mel. The putative bidirectional regulation of sleep behavior through the BK channel might also exist in mammals, although the signaling molecule is perhaps norepinephrine instead of octopamine because norepinephrine, which is a vertebrate equivalent of octopamine (48), has a wake-promoting effect in vertebrates (49, 50).

G proteins are trimeric complexes of Gα, Gβ, and Gγ subunits. Before the activation of a GPCR, the three subunits are closely associated with GDP bound to the Gα subunit. Upon activation of the GPCR, a substitution of GDP by GTP in the Gα subunit causes dissociation of the G protein into Gα-GTP and free Gβγ subunits, which can produce their biological effects independently. A variety of ion channels are regulated either directly or indirectly by Gβγ, including G protein-gated inward rectifier K^+ (GIRK) channels (51), TRP channels (52, 53), piezo channels (54), and voltage-gated Ca^{2+} channels (55). Mechanistically, the regulation of GIRK channels by Gβγ is best understood. Gβγ binds to GIRK channels to activate them through a membrane-delimited mechanism (51, 56–58). In the present study, we show that induction of free Gβγ by mSIRK augments hSlo1 activity whereas inhibition of Gβγ by gallein inhibits hSlo1 activity. The result with gallein is in agreement with that of a very recent study showing that gallein can eliminate a stimulating effect of propionate, a short-chain fatty acid, on the BK channel in arterial smooth muscle cells (59). The opposite effects of gallein and mSIRK on hSlo1 indicate that Gβγ subunits likely mediate the activating effect of Mel.

This study offers insights to some reported effects of exogenous Mel on *C. elegans*. For example, one study showed that exogenous Mel has a strong inhibitory effect on worm locomotion (24). This effect of Mel resembles those of ethanol

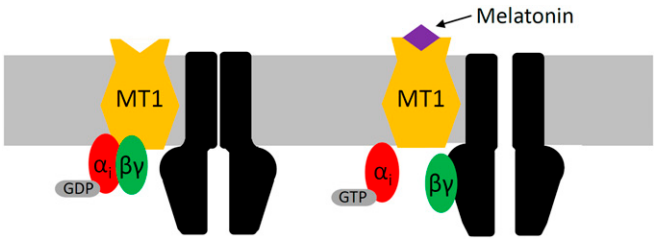

Fig. 7. Model of BK channel activation by Mel. Binding of Mel to MT_1 causes the exchange of GDP by GTP in the α subunit of a Gi-type G protein, the dissociation of the trimeric G protein into G_iα-GTP and Gβγ subunits, and the binding of free Gβγ subunits to the BK channel to cause channel activation.

intoxication (60) and *slo-1* gain-of-function mutation (26) but its molecular mechanism is unknown. The results of this study suggest that, like the intoxicating effect of ethanol (60), SLO-1 activation in neurons is likely a major mechanism for the inhibitory effect of Mel on locomotion. Another study showed that treatment of dystrophin (*dys-1*) mutant worms with exogenous Mel improves muscular strength, thrashing rate, and mitochondrial integrity (61). Although Mel has also been used to treat muscular dystrophy patients (62), the molecular mechanism for its beneficial muscle effects is unknown. Given that *dys-1* deficiencies enhance cholinergic synaptic transmission (63) and that the *dys-1*-associated protein complex plays a pivotal role in neuronal SLO-1 function by localizing SLO-1 to presynaptic sites (28, 64–66), activation of neuronal SLO-1 might be partially responsible for the beneficial effects of Mel in *dys-1*-deficient worms.

To summarize, the present study shows that the BK channel is a key molecular target that Mel may act on to produce its sleep-promoting effect and that hSlo1 can also be activated by Mel in a MT_1-dependent manner. These findings suggest that the BK channel might play an evolutionarily conserved role in Mel's sleep-promoting effect. Investigations into this possibility in mammals will likely lead to major advances in our understanding about sleep biology.

Materials and Methods

***C. elegans* Culture and Strains.** *C. elegans* were raised on nematode growth medium plates with a layer of OP50 *E. coli* at 22 °C inside an environmental chamber. The strains used are described in the *SI Appendix*.

Generation of the homt-1 Mutant. *homt-1* knockout worms were generated using the CRISPR/Cas9 approach. Details are described in the *SI Appendix*.

Analysis of Expression Pattern and Subcellular Localization. The expression patterns of *pcdr-1* and *homt-1* were assessed by expressing GFP under the control of their promoters. Subcellular localization of PCDR-1 in the neuron was determined by fusing GFP to its carboxyl terminus and expressing the fusion protein under the control of *Prab-3*. Details are provided in the *SI Appendix*.

***C. elegans* Electrophysiology.** All electrophysiological experiments were performed with adult hermaphrodites maintained in a low-temperature incubator at 22 °C. ePSCs and minis at the *C. elegans* neuromuscular junction were recorded as described previously (31, 67). Further information may be found in the *SI Appendix*.

***Xenopus* Oocyte Electrophysiology.** *Xenopus* oocytes were used to examine the effects of Mel receptors on hSlo1 function. Further information may be found in the *SI Appendix*.

Sleep Behavior Analysis. Mid-L4 stage worms were individually placed inside the openings of a polydimethylsiloxane (PDMS) membrane and imaged at 10-s intervals for 10 h. Image acquisition and subsequent analyses were performed using a custom-written program running in Matlab, which may be accessed at GitHub: https://github.com/WanglabNiu/PNAS_sleep-tracking-software. Further information may be found in the *SI Appendix*.

Statistical Analyses. Amplitudes of currents, frequencies of minis, and open probability of single-channel events were quantified using the ClampFit software. Dwell time analyses were performed using OriginPro (version 2020, OriginLab, Northampton, MA, USA). Data graphing and statistical analyses were performed with OriginPro. All data are shown as mean ± SE. The sample size (*n*) equals the number of worms or membrane patches recorded. Further information may be found in the *SI Appendix*.

Data Availability. All study data are included in the article and *SI Appendix*.

ACKNOWLEDGMENTS. We thank Liam Connelly for creating a CAD file for the PDMS membrane, Adam Adler for advice on statistical analyses, and the Caenorhabditis Genetics Center (USA) for worm strains. This work was supported by NIH (R01MH085927, R01NS109388, to Z.-W.W.; R01GM113004 to B.C.).

1. D. C. Fernandez, Y. T. Chang, S. Hattar, S. K. Chen, Architecture of retinal projections to the central circadian pacemaker. *Proc. Natl. Acad. Sci. U.S.A.* **113**, 6047–6052 (2016).
2. J. Cipolla-Neto, F. G. D. Amaral, Melatonin as a hormone: New physiological and clinical insights. *Endocr. Rev.* **39**, 990–1028 (2018).
3. J. Liu *et al.*, MT1 and MT2 melatonin receptors: A therapeutic perspective. *Annu. Rev. Pharmacol. Toxicol.* **56**, 361–383 (2016).
4. R. Jockers *et al.*, Update on melatonin receptors: IUPHAR review 20. *Br. J. Pharmacol.* **173**, 2702–2725 (2016).
5. S. Comai, R. Ochoa-Sanchez, G. Gobbi, Sleep-wake characterization of double MT_1/MT_2 receptor knockout mice and comparison with MT_1 and MT_2 receptor knockout mice. *Behav. Brain Res.* **243**, 231–238 (2013).
6. C. von Gall *et al.*, Rhythmic gene expression in pituitary depends on heterologous sensitization by the neurohormone melatonin. *Nat. Neurosci.* **5**, 234–238 (2002).
7. A. Jilg *et al.*, Rhythms in clock proteins in the mouse pars tuberalis depend on MT1 melatonin receptor signalling. *Eur. J. Neurosci.* **22**, 2845–2854 (2005).
8. G. Gobbi, S. Comai, Differential function of melatonin MT_1 and MT_2 receptors in REM and NREM sleep. *Front. Endocrinol. (Lausanne)* **10**, 87 (2019).
9. M. L. Dubocovich *et al.*, International Union of basic and clinical pharmacology. LXXV. Nomenclature, classification, and pharmacology of G protein-coupled melatonin receptors. *Pharmacol. Rev.* **62**, 343–380 (2010).
10. A. Benleulmi-Chaachoua *et al.*, Protein interactome mining defines melatonin MT1 receptors as integral component of presynaptic protein complexes of neurons. *J. Pineal Res.* **60**, 95–108 (2016).
11. M. Griguoli, M. Sgritta, E. Cherubini, Presynaptic BK channels control transmitter release: Physiological relevance and potential therapeutic implications. *J. Physiol.* **594**, 3489–3500 (2016).
12. L. O. Trussell, M. T. Roberts, "The role of potassium channels in the regulation of neurotransmitter release" in *in Molecular Mechanisms of Neurotransmitter Release*, Z. W. Wang, Ed. (Humana Press, Totowa, NJ, 2008), pp. 171–185.
13. Z. W. Wang, Regulation of synaptic transmission by presynaptic CaMKII and BK channels. *Mol. Neurobiol.* **38**, 153–166 (2008).
14. S. Panda *et al.*, Coordinated transcription of key pathways in the mouse by the circadian clock. *Cell* **109**, 307–320 (2002).
15. A. L. Meredith *et al.*, BK calcium-activated potassium channels regulate circadian behavioral rhythms and pacemaker output. *Nat. Neurosci.* **9**, 1041–1049 (2006).
16. H. Mizutani *et al.*, Modulation of Ca2+ oscillation and melatonin secretion by BKCa channel activity in rat pinealocytes. *Am. J. Physiol. Cell Physiol.* **310**, C740–C747 (2016).
17. A. Crocker, M. Shahidullah, I. B. Levitan, A. Sehgal, Identification of a neural circuit that underlies the effects of octopamine on sleep:wake behavior. *Neuron* **65**, 670–681 (2010).
18. N. F. Trojanowski, D. M. Raizen, Call it worm sleep. *Trends Neurosci.* **39**, 54–62 (2016).
19. D. M. Raizen *et al.*, Lethargus is a Caenorhabditis elegans sleep-like state. *Nature* **451**, 569–572 (2008).
20. M. Jeon, H. F. Gardner, E. A. Miller, J. Deshler, A. E. Rougvie, Similarity of the C. elegans developmental timing protein LIN-42 to circadian rhythm proteins. *Science* **286**, 1141–1146 (1999).
21. C. Cirelli, The genetic and molecular regulation of sleep: From fruit flies to humans. *Nat. Rev. Neurosci.* **10**, 549–560 (2009).
22. M. D. Nelson, D. M. Raizen, A sleep state during C. elegans development. *Curr. Opin. Neurobiol.* **23**, 824–830 (2013).
23. A. Sehgal, E. Mignot, Genetics of sleep and sleep disorders. *Cell* **146**, 194–207 (2011).
24. D. Tanaka, K. Furusawa, K. Kameyama, H. Okamoto, M. Doi, Melatonin signaling regulates locomotion behavior and homeostatic states through distinct receptor pathways in Caenorhabditis elegans. *Neuropharmacology* **53**, 157–168 (2007).
25. C. D. Keating *et al.*, Whole-genome analysis of 60 G protein-coupled receptors in Caenorhabditis elegans by gene knockout with RNAi. *Curr. Biol.* **13**, 1715–1720 (2003).
26. B. Chen *et al.*, A novel auxiliary subunit critical to BK channel function in *Caenorhabditis elegans*. *J. Neurosci.* **30**, 16651–16661 (2010).

27. B. Chen *et al*., α-Catulin CTN-1 is required for BK channel subcellular localization in *C. elegans* body-wall muscle cells. *EMBO J.* **29**, 3184–3195 (2010).
28. B. Chen, P. Liu, H. Zhan, Z. W. Wang, Dystrobrevin controls neurotransmitter release and muscle $Ca^{(2+)}$ transients by localizing BK channels in *Caenorhabditis elegans*. *J. Neurosci.* **31**, 17338–17347 (2011).
29. D. X. Tan, L. C. Manchester, E. Sanchez-Barcelo, M. D. Mediavilla, R. J. Reiter, Significance of high levels of endogenous melatonin in Mammalian cerebrospinal fluid and in the central nervous system. *Curr. Neuropharmacol.* **8**, 162–167 (2010).
30. A. Anderson, Y. L. Chew, W. Schafer, R. McMullan, Identification of a conserved, orphan G protein-coupled receptor required for efficient pathogen clearance in Caenorhabditis elegans. *Infect. Immun.* **87**, e00034-19 (2019).
31. Z. W. Wang, O. Saifee, M. L. Nonet, L. Salkoff, SLO-1 potassium channels control quantal content of neurotransmitter release at the *C. elegans* neuromuscular junction. *Neuron* **32**, 867–881 (2001).
32. M. L. Migliori *et al*., Daily variation in melatonin synthesis and arylalkylamine N-acetyltransferase activity in the nematode Caenorhabditis elegans. *J. Pineal Res.* **53**, 38–46 (2012).
33. J. Borjigin, X. Li, S. H. Snyder, The pineal gland and melatonin: Molecular and pharmacologic regulation. *Annu. Rev. Pharmacol. Toxicol.* **39**, 53–65 (1999).
34. K. Schuske, A. A. Beg, E. M. Jorgensen, The GABA nervous system in C. elegans. *Trends Neurosci.* **27**, 407–414 (2004).
35. L. R. Varshney, B. L. Chen, E. Paniagua, D. H. Hall, D. B. Chklovskii, Structural properties of the *Caenorhabditis elegans* neuronal network. *PLoS Comput. Biol.* **7**, e1001066 (2011).
36. A. Yuan *et al*., SLO-2, a K^+ channel with an unusual Cl^- dependence. *Nat. Neurosci.* **3**, 771–779 (2000).
37. P. Liu, B. Chen, Z. W. Wang, SLO-2 potassium channel is an important regulator of neurotransmitter release in Caenorhabditis elegans. *Nat. Commun.* **5**, 5155 (2014).
38. A. Wei *et al*., Efficient isolation of targeted *Caenorhabditis elegans* deletion strains using highly thermostable restriction endonucleases and PCR. *Nucleic Acids Res.* **30**, e110 (2002).
39. F. Goubaeva *et al*., Stimulation of cellular signaling and G protein subunit dissociation by G protein betagamma subunit-binding peptides. *J. Biol. Chem.* **278**, 19634–19641 (2003).
40. D. M. Lehmann, A. M. Seneviratne, A. V. Smrcka, Small molecule disruption of G protein beta gamma subunit signaling inhibits neutrophil chemotaxis and inflammation. *Mol. Pharmacol.* **73**, 410–418 (2008).
41. K. Ukhanov, D. Brunert, E. A. Corey, B. W. Ache, Phosphoinositide 3-kinase-dependent antagonism in mammalian olfactory receptor neurons. *J. Neurosci.* **31**, 273–280 (2011).
42. A. L. A. Nichols, T. Eichler, R. Latham, M. Zimmer, A global brain state underlies *C. elegans* sleep behavior. *Science* **356**, eaam6851 (2017).
43. M. Turek, I. Lewandrowski, H. Bringmann, An AP2 transcription factor is required for a sleep-active neuron to induce sleep-like quiescence in C. elegans. *Curr. Biol.* **23**, 2215–2223 (2013).
44. W. Steuer Costa *et al*., A GABAergic and peptidergic sleep neuron as a locomotion stop neuron with compartmentalized Ca2+ dynamics. *Nat. Commun.* **10**, 4095 (2019).
45. E. Maluck *et al*., A wake-active locomotion circuit depolarizes a sleep-active neuron to switch on sleep. *PLoS Biol.* **18**, e3000361 (2020).
46. S. Choi, M. Chatzigeorgiou, K. P. Taylor, W. R. Schafer, J. M. Kaplan, Analysis of NPR-1 reveals a circuit mechanism for behavioral quiescence in C. elegans. *Neuron* **78**, 869–880 (2013).
47. D. L. Chase, M. R. Koelle, Biogenic amine neurotransmitters in C. elegans. *WormBook*, 1–15 (2007).
48. P. Bauknecht, G. Jékely, Ancient coexistence of norepinephrine, tyramine, and octopamine signaling in bilaterians. *BMC Biol.* **15**, 6 (2017).
49. C. Singh, G. Oikonomou, D. A. Prober, Norepinephrine is required to promote wakefulness and for hypocretin-induced arousal in zebrafish. *eLife* **4**, e07000 (2015).
50. C. W. Berridge, B. E. Schmeichel, R. A. España, Noradrenergic modulation of wakefulness/arousal. *Sleep Med. Rev.* **16**, 187–197 (2012).
51. M. R. Whorton, R. MacKinnon, X-ray structure of the mammalian GIRK2-βγ G-protein complex. *Nature* **498**, 190–197 (2013).
52. Y. Shen, M. A. Rampino, R. C. Carroll, S. Nawy, G-protein-mediated inhibition of the Trp channel TRPM1 requires the Gβγ dimer. *Proc. Natl. Acad. Sci. U.S.A.* **109**, 8752–8757 (2012).
53. O. Alkhatib *et al*., Promiscuous G-protein-coupled receptor inhibition of transient receptor potential melastatin 3 ion channels by Gβγ subunits. *J. Neurosci.* **39**, 7840–7852 (2019).
54. J. S. Del Rosario *et al*., Gi-coupled receptor activation potentiates Piezo2 currents via Gβγ. *EMBO Rep.* **21**, e49124 (2020).
55. K. P. Currie, G protein modulation of CaV2 voltage-gated calcium channels. *Channels (Austin)* **4**, 497–509 (2010).
56. G. Krapivinsky, L. Krapivinsky, K. Wickman, D. E. Clapham, G beta gamma binds directly to the G protein-gated K+ channel, IKACh. *J. Biol. Chem.* **270**, 29059–29062 (1995).
57. W. Wang, M. R. Whorton, R. MacKinnon, Quantitative analysis of mammalian GIRK2 channel regulation by G proteins, the signaling lipid PIP2 and Na+ in a reconstituted system. *eLife* **3**, e03671 (2014).
58. C. Lüscher, P. A. Slesinger, Emerging roles for G protein-gated inwardly rectifying potassium (GIRK) channels in health and disease. *Nat. Rev. Neurosci.* **11**, 301–315 (2010).
59. W. Zhang *et al*., Prenatal hypoxia inhibited propionate-evoked BK channels of mesenteric artery smooth muscle cells in offspring. *J. Cell. Mol. Med.* **24**, 3192–3202 (2020).
60. A. G. Davies *et al*., A central role of the BK potassium channel in behavioral responses to ethanol in C. elegans. *Cell* **115**, 655–666 (2003).
61. J. E. Hewitt *et al*., Muscle strength deficiency and mitochondrial dysfunction in a muscular dystrophy model of *Caenorhabditis elegans* and its functional response to drugs. *Dis. Model. Mech.* **11**, dmm036137 (2018).
62. M. Chahbouni *et al*., Melatonin treatment normalizes plasma pro-inflammatory cytokines and nitrosative/oxidative stress in patients suffering from Duchenne muscular dystrophy. *J. Pineal Res.* **48**, 282–289 (2010).
63. C. Bessou, J. B. Giugia, C. J. Franks, L. Holden-Dye, L. Ségalat, Mutations in the Caenorhabditis elegans dystrophin-like gene dys-1 lead to hyperactivity and suggest a link with cholinergic transmission. *Neurogenetics* **2**, 61–72 (1998).
64. H. Kim *et al*., The dystrophin complex controls bk channel localization and muscle activity in *Caenorhabditis elegans*. *PLoS Genet.* **5**, e1000780 (2009).
65. K. H. Oh *et al*., Presynaptic BK channel localization is dependent on the hierarchical organization of alpha-catulin and dystrobrevin and fine-tuned by CaV2 calcium channels. *BMC Neurosci.* **16**, 26 (2015).
66. F. Sancar *et al*., The dystrophin-associated protein complex maintains muscle excitability by regulating Ca(2+)-dependent K(+) (BK) channel localization. *J. Biol. Chem.* **286**, 33501–33510 (2011).
67. Q. Liu *et al*., Presynaptic ryanodine receptors are required for normal quantal size at the *Caenorhabditis elegans* neuromuscular junction. *J. Neurosci.* **25**, 6745–6754 (2005).